A MODEL FOR ESTIMATING THE LATERAL OVERLAP PROBABILITY OF AIRCRAFT WITH RNP ALERTING CAPABILITY IN PARALLEL RNAV ROUTES

Sakae NAGAOKA*
***Electronic Navigation Research Institute/The University of Tokyo**

Keywords: *collision risk, RNP, overlap probability, RNAV*

Abstract

The Lateral overlap probability is a critical parameter for estimating the collision risk of aircraft pairs flying on parallel tracks. This is usually estimated from the distribution models of cross track errors. As a model of the distribution, a mixed probability density function (pdf) model consisting of the generalized Laplace (GL) core and double exponential (DE) tail is proposed in this paper. Based on this model, the characteristics of the distribution are discussed in relation to the maximum lateral overlap probability. In addition to this, simple expressions of maximum lateral overlap probability for an aircraft with RNP alerting capability flying on parallel tracks are indicated in this paper.

1 Introduction

Most modern RNAV (Area Navigation) system provides on board performance monitoring and alerting. The navigation specifications developed for use by these systems are currently designated RNP (Required Navigation Performance) [1]. The concept of RNP has changed significantly in the past ten years [1],[2]. For simplicity, we discuss the problem on the framework of the RNP manual [2].

In Ref. [2], RNP is one of the key factors in the determination of separation minima used in the airspace where an RNP type is specified. The RNP type was defined only in terms of navigation performance accuracy [2], which was specified as a limit where total system error (TSE) must not exceed for 95% of flight time.

RNP RNAV was the term to describe systems that were compliant with the requirements of the MASPS [3] in addition to the accuracy requirement. This is currently mentioned as RNP. The containment integrity was specified by the maximum allowable probability for the event that TSE is greater than the containment limit (2 × RNP value) and the condition has not been detected. The probability is 10^{-5}/hr.

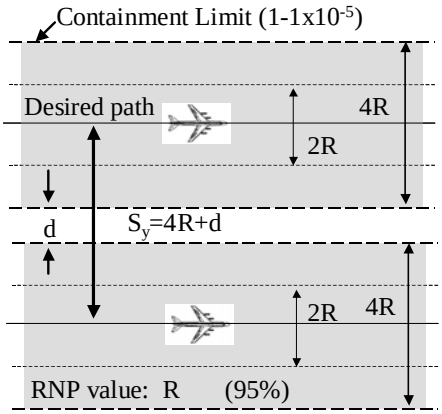

Fig.1 Configuration of parallel route.

Fig.1 shows the configuration of parallel route for RNP RNAV aircraft. The centerline corresponds to the desired path.

It seems to be reasonable for us to determine the route spacing on the basis of collision risk assessment. The lateral overlap probability is one of the key parameters of the collision risk model. This is usually estimated from the distribution of cross track errors of aircraft flying on the tracks under consideration. The shape of cross track error distribution for RNP RNAV aircraft may be constrained by two conditions, one is the 95% accuracy (RNP

value) and the other is related to the containment limit. Though we have no empirical distribution of cross track errors at present, we may estimate a maximum lateral overlap probability for the RNP RNAV aircraft taking into account the conditions.

In the previous papers [4][5], the lateral overlap probability of RNP RNAV aircraft flying on parallel tracks was estimated on the basis of TSE (or cross track error) distribution models taking into account both the 95% accuracy and containment integrity. Models of the probability density functions describing the distributions of cross track errors have been proposed. The models describing the distributions of the core region and that for tail region were assumed separately. The models assumed the Gaussian-like core and the double exponential or uniform tail. Under several assumptions the characteristics of the lateral overlap probability for RNP RNAV parallel tracks have been investigated.

However, the proposed models[3][4] have resulted in discontinuity in its probability density at a point associated with the containment limit. In order to avoid this unnaturalness, a continuous probability density function model composed of a mixture of two distribution models is proposed in this paper. In the new model, a mixture of the generalized Laplace(GL) distribution and double exponential(DE) distribution is used for describing the probability density function of cross track errors.

This paper firstly describes the methods of modeling the distribution and estimating the maximum lateral overlap probability. Then examples of numerical calculation are shown. Finally, simple expressions for calculating the maximum lateral overlap probability are derived.

3. Capability of RNP RNAV Aircraft

An RNP RNAV equipped aircraft system alerts the pilot when the TSE exceeds the containment limit. Fig.2 shows the possible states of the navigational system of an RNP RNAV equipped aircraft. . The states are as follows

E1: |TSE|<2R and no alert of loss of RNP capability

E2: |TSE|>2R and no alert of loss of RNP capability

E3: Alert of loss of RNP capability

where R is the RNP value (the 95% accuracy requirement).

The frequency of large cross track error (TSE) of RNP RNAV aircraft will be reduced significantly due to the alerting capability. The pilot can take remedial actions when the system issues an alert of loss of RNP capability. Finally, in most cases (E1 and E3) the TSE will be bounded within the interval [-2R,2R]. Only the case of E2 allows large cross track errors beyond the containment limit.

In the following sections, we consider the lateral overlap probability of RNP RNAV aircraft flying on parallel tracks under several assumptions. The schematic view of the tracks under consideration is shown in Fig.1.

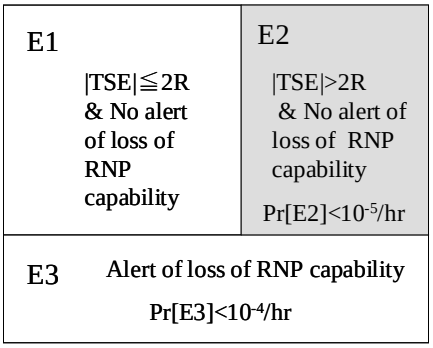

Fig.2 Probability of each event [3]

3 Models of Cross Track Errors

3.1 Requirements for Probability Density Function

Let us denote the probability density function (pdf) of the cross track error, X, of RNP-RNAV aircraft by $f(x)$. The probability distribution function F(x) is defined by

$$F(x) = \int_{-\infty}^{x} f(x)dx \qquad (1)$$

From the 95% containment for RNP value, R satisfies

$$F(R) - F(-R) \geq 1 - 0.05 \qquad (2)$$

From the requirement for the containment limit, let the probability that |x|>2R be γ_2 (=

10^{-5}) assuming that the average flight period of deviated aircraft without the alert of RNP capability is one hour. Then, the requirement for the distribution function is given by

$$F(2R) - F(-2R) \geq 1 - \gamma_2 \qquad (3)$$

Herein, the pdf, $f(x)$ satisfies

$$F(\infty) = \int_{-\infty}^{\infty} f(x)dx = 1 \qquad (4)$$

In this paper we solely consider the case that the equalities in Eq.(2) and Eq.(3) are satisfied as a simple example. In the previous papers [4],[5], separate models were defined to satisfy the constraints (2) and (3). This resulted in discontinuity at |X| = 2R. In this paper, we consider a continuous mixture distribution as shown in Fig3.

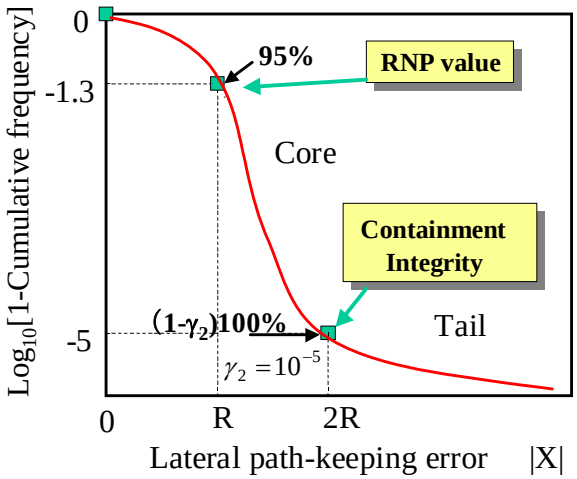

Fig.3 Required positions on the distribution.

3.2 Model of Probability Density Function

Let us assume the pdf of the cross track error X, $f(x)$, has the following characteristics.

(i) zero mean and symmetric around X=0.

(ii) unimodal (has a unique peak at X=0)

(iii) most heavily weighted in the core region ($|X| < K$), $K(<2R)$ is an appropriate value) and slowly varying in magnitude in the tail ($|X| > K$) region.

Herein, we assume the following continuous mixture distribution

$$f(x) = (1-\alpha) f_c(x) + \alpha \cdot f_t(x) \qquad (5)$$

where α is the weighting coefficient associated with the tail region ($0 < \alpha << 1$). $f_c(x)$ and $f_t(t)$ are the pdfs associated with the core and tail, respectively.

3.3 Model for Core Distribution

As the candidate of the $f_c(x)$, the generalized Laplace (GL) distribution may be appropriate because it changes the shape according to choice of the shape parameter. The pdf of the GL distribution is given by

$$f_c(x) = (2ab\Gamma(b))^{-1} \exp(-|x/a|^{1/b}) \qquad (6)$$

where $a(>0)$ is the scale parameter, $b(>0)$ the shape parameter and $\Gamma(b)$ is the Gamma function which is defined by

$$\Gamma(b) = \int_0^{\infty} t^{b-1} \exp(-t)dt \qquad (7)$$

The shape of the GL distribution varies with its shape parameter b. In the case of $b=1$, Eq.(6) becomes the double exponential (DE) distribution. The case of $b=0.5$ corresponds to the normal (or Gaussian) distribution. Fig.4 shows the shape of GL distribution for different shape parameter values. The previous papers [4],[5] indicated that the weighting coefficient $1-\alpha$ of $f_c(x)$ for the Gaussian is greater than 1. This fact contradicts with the condition $0 < \alpha << 1$. This suggests that the value of b which meets the distribution requirements described in Section 3.1 must be less than 0.5.

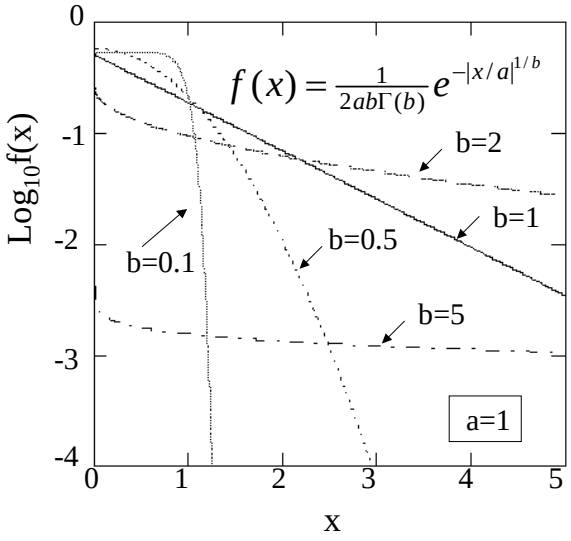

Fig.4 Shapes of GL distribution (a=1) for different shape parameter values.

3.4 Distribution Model for Tail Region

As mentioned in 3.2, we assume a distribution which decreases slowly with the magnitude of the cross track error and which is very low in the tail region. Though it is not impossible to assume the GL distribution for the tail, it increases the complexity of analysis significantly because of too many model parameters. Therefore, let us assume the DE tail as used in the previous paper [5].

$$f_t(x) = (2\lambda)^{-1} \exp(-|x|/\lambda) \quad (8)$$

where λ (>0) is the scale parameter.

4. Lateral Overlap Probability

Let us consider the aircraft pairs flying on the parallel tracks of which track spacing is S_y at the same flight level as shown in Fig.1. The lateral overlap probability of aircraft pairs is given by

$$P_y(S_y) = \int_{S_y-\lambda_y}^{S_y+\lambda_y} C(z)dz \quad (9)$$

where λ_y is the average wing span of aircraft, and

$$C(z) \equiv \int_{-\infty}^{\infty} f(x) f(x-z)dx \quad (10)$$

is the lateral overlap density function.

Herein, the track spacing S_y is assumed to be S_y=4R+d. d(≥ 0) is the distance between the containment limits and λ_y =0.0321NM(=59m). Under the assumption of 3.2, the following approximation[6] can be used

$$C(S_y) \approx 2 f(S_y) \quad (11)$$

At about $z = S_y$, by the assumption (iii) and Eq.(11), $C(z)$ varies very slowly. Then, the following approximation can be made

$$P_y(S_y) \approx 2\lambda_y C(S_y) \quad (12)$$

Finally, we obtain

$$P_y(S_y) \approx 4\lambda_y \cdot f(S_y) \quad (13)$$

5 Solving Equations

First of all, we have to obtain the parameters of $f(x)$ which satisfies the equalities in Eq.(2) and Eq.(3) simultaneously. In the GL-DE mixture model, there are four parameters

$$f(x) = f(x|a,b,\lambda,\alpha) \quad (14)$$

On the other hand, since the number of equations is two, the parameters cannot be determined uniquely. Therefore, we look for a set of parameters, which approximately maximizes the lateral overlap probability.

Let us consider the probability density at $z = S_y$

$$f(S_y) = (1-\alpha) f_c(S_y) + \alpha \cdot f_t(S_y) \quad (15)$$

Herein, $f_c(S_y) << f_t(S_y)$ for $S_y \geq 2R$ and $0 < \alpha << 1$. Then, we can use the following approximation.

$$P_y(S_y) \approx 4\lambda_y f(S_y) \approx 4\lambda_y \alpha \cdot f_t(S_y) \quad (16)$$

$$= \frac{4\lambda_y \alpha}{2\lambda} \exp(-S_y/\lambda) \quad (17)$$

Eq.(17) increases monotonically with α if α is independent of λ. The condition of maximization with respect to λ is given by

$$\partial P_y(S_y)/\partial\lambda = 0 \quad (18)$$

for $\lambda = S_y$, Eq.(17) becomes maximal.

$$P_y(S_y) \approx (2\lambda_y \alpha / S_y) \cdot e^{-1} \quad (19)$$

However, in our case α is a function of λ and dependent on it as described later.

6. Determination of Parameters

The conditions of equalities in Eq.(2) and Eq.(3) for the mixture distribution can be rewritten as

$$(1-\alpha) I_{c,1} + \alpha I_{t,1} = 1 - 0.05 \quad (20)$$

$$(1-\alpha) I_{c,2} + \alpha I_{t,2} = 1 - \gamma_2 \quad (21)$$

where

$$I_{c,m} = \int_{-mR}^{mR} f_c(x)dx \quad (m=1,2) \quad (22)$$

$$I_{t,m} = \int_{-mR}^{mR} f_t(x)dx \quad (m=1,2) \quad (23)$$

For the GL core and DE tail models, we obtain

$$I_{t,m} = 1 - e^{-mR/\lambda} \quad (24)$$

$$I_{c,m} = \int_{-mR}^{mR} [2ab\Gamma(b)]^{-1} e^{-|x/a|^{1/b}} dx \quad (25)$$

For the convenience of dealing with x, let us normalize the following quantities with the RNP value R.

$$x = k_x R \quad (26)$$

$$a = k_a R \quad (27)$$

$$\lambda = k_l R \quad (28)$$

where k_x , k_a and k_l are the normalized (dimensionless) cross track error, scale parameter of GL model and that of DE model, respectively. Using these, we obtain

$$I_{t,m} = 1 - e^{-m/k_l} \quad (29)$$

$$I_{c,m} = \int_{-m}^{m} (2k_a b\Gamma(b))^{-1} e^{-|k_x/k_a|^{1/b}} dk_x \quad (30)$$

We deal with the problem of maximizing a function consisting of four parameters, k_a, b, k_l, α . Eliminating α from Eq.(20) and Eq.(21) under a given k_l , we obtain the following equation

$$G(k_a, b, k_l) \equiv (I_{c,2} - 1 + e^{-2/k_l})(I_{c,1} - (1 - 0.05)) - (I_{c,2} - (1 - \gamma_2))(I_{c,1} - 1 + e^{-1/k_l}) = 0 \quad (31)$$

Once b and k_l are given, $k_a = k_a(b, k_l)$ can be obtained by solving the above equation. Then, α can be calculated by

$$\alpha(b, k_l) = (I_{c,1} - (1 - 0.05)) / (I_{c,1} - (1 - e^{-1/k_l})) \quad (32)$$

7 Examples of Calculation

7.1 Method of Solving Equations

Firstly, let the tail parameter be $\lambda = k_l R$ with k_l =4. Secondly, we set a value for b. Thirdly we obtain solutions of k_a which satisfy Eq.(31) numerically by the Newton method. Then we calculate the candidates of the solution for α ($0 < \alpha < 1$) using Eq.(32). The set of solutions can be obtained by the above-mentioned procedures. Among these solutions, the set which maximizes $P_y(S_y)$ would be the final solution. The calculation was made by a mathematical software package called MATHCAD.

Fig.5 indicates an example of evaluated values of the function $G(k_a, 0.1, 4)$ for b =0.1 and $k_l = 4$. Solutions for k_a can be seen at approximately 1 and 6. The substitution of solutions of $k_a(b)$ obtained from Eq.(31) for Eq.(32) yields the possible α values. If the calculated α exists within (0,1) , it would be an effective solution.

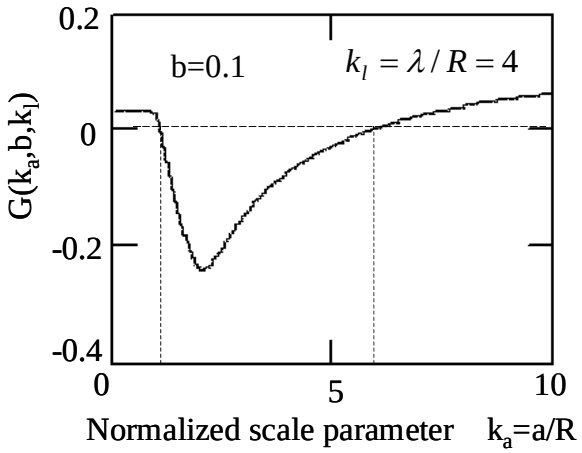

Fig.5 Possible solutions of k_a for a given b(=0.1). $\lambda = S = 4R$.

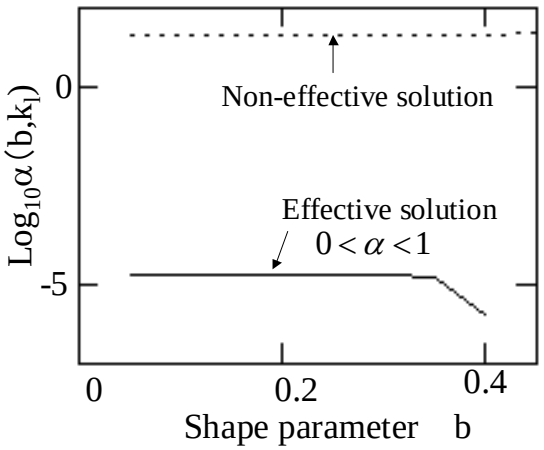

Fig.6 Possible solutions for α . $k_l = \lambda / R = 4$.

Fig.6 plots the solutions of $\alpha = \alpha(b, k_l)$ for various values of b . b is changed discretely within [0.05,0.45] by each 0.05 interval. In this case, we took $\lambda = 4R$. As seen in the figure, the effective solution ($0 < \alpha < 1$) can be obtained for the region where b is up to a value between 0.40 and 0.45. Detailed numerical computation showed that an effective solution existed until $b = 0.40275$. In the region where b is smaller than a value of about 0.3, the value of α asymptotically approaches to a value. No effective solution exists at $b = 0.5$. This means that it is impossible to fit the mixed distribution by the Gaussian core.

Fig.7 shows examples of distributions by solutions for various values of b when $k_l = 4$. The cases for $b = 0.1$, 0.3 and 0.4 are indicated. α looks constant for small values of b and starts decreasing at about $b = 0.3$. Since $f_{t(}x)$ >>

$f_c(x)$ and since the tail probability does not depend on b, one can expect that the mixture probability for large deviations is a function of alpha alone. This is why the tail probabilities for b<0.3 seem to have equal values. Fig.8 shows the similar distributions for the case $k_l = 5$.

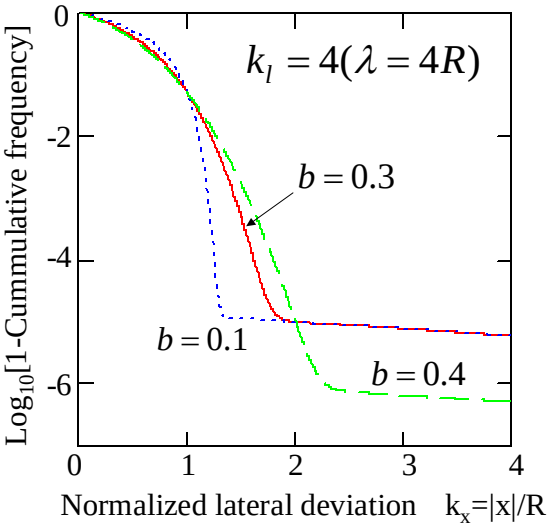

Fig.7 Mixture distribution for $\lambda = 4R$.

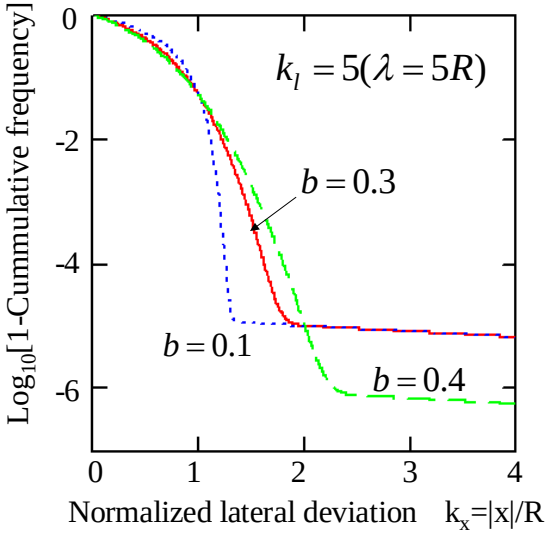

Fig.8 Mixture distribution for $\lambda = 5R$.

7.2 Maximum value for $P_y(S_y)$

From Eq.(21), α can be obtained by

$$\alpha = \frac{1 - \gamma_2 - I_{c,2}}{I_{t,2} - I_{c,2}} \qquad (33)$$

where

$$I_{c,2} = 1 - 2\int_{2R}^{\infty} f_c(x)dx \qquad (34)$$

and

$$I_{t,2} = 1 - 2\int_{2R}^{\infty} f_t(x)dx \qquad (35)$$

Using Eq.(34) and Eq.(35), Eq.(33) can be rewritten as

$$\alpha = \frac{\gamma_2 - 2\int_{2R}^{\infty} f_c(x)dx}{2(\int_{2R}^{\infty} f_t(x)dx - \int_{2R}^{\infty} f_c(x)dx)} \qquad (36)$$

As seen in Fig.7 and Fig.8, the core rapidly decreases in the region $1 < k_x < 2$ (R<x<2R) as the shape parameter b deceases from about 0.3. In the region $k_x > 2$, i.e., x>2R, the relation $f_c(x) << f_t(x)$ would be satisfied. Then, α becomes a function of λ, independent of b, if $\int_{2R}^{\infty} f_c(x)dx$ is negligibly small compared to γ_2 and $\int_{2R}^{\infty} f_t(x)dx$. The estimate of α, namely, α_0 can be approximated by

$$\alpha_0 = \gamma_2 / [2\int_{2R}^{\infty} f_t(x)dx] \qquad (37)$$

Substituting the DE tail model into Eq.(37), we obtain

$$\alpha_0 = \gamma_2 \cdot e^{2R/\lambda} \qquad (38)$$

The conditions $0 < a < 1$ are fulfilled for any choice of $\lambda > 0$.

Substituting Eq.(38) for α of Eq.(17), we obtain

$$P_y(S_y) \approx 2\lambda_y \frac{\gamma_2 \cdot e^{-(S_y - 2R)/\lambda}}{\lambda} \qquad (39)$$

From the condition $\partial P_y(S_y)/\partial\lambda = 0$, we can see that Eq.(39) has a local maximum at $\lambda = S_y - 2R$ (assuming $S_y \geq 4R$). The maximum lateral overlap probability for the DE tail model, $P_y(S_y)_{DE}$ can be given by

$$P_y(S_y)_{DE} \approx 2\lambda_y \frac{\gamma_2 \cdot e^{-1}}{S_y - 2R} \qquad (40)$$

7.3 Example of Calculated $P_y(S_y)$

Fig.9 plots the quantities, i.e., $q_1 \equiv f_t(S_y, \lambda)$, $q_2 \equiv \alpha_{\max}(\lambda)$, and $q_3 \equiv P_y(S_y, \lambda)$ as a function of the DE tail parameter λ for the case $S_y = 4R$ and R=1NM. As shown in the figure, q_1 becomes maximal at $k_l = 4$ ($\lambda = S_y$) (not visible) and q_3 has a maximum at $k_l = 2$ (λ=Sy-2R) as shown in Section 7.2.

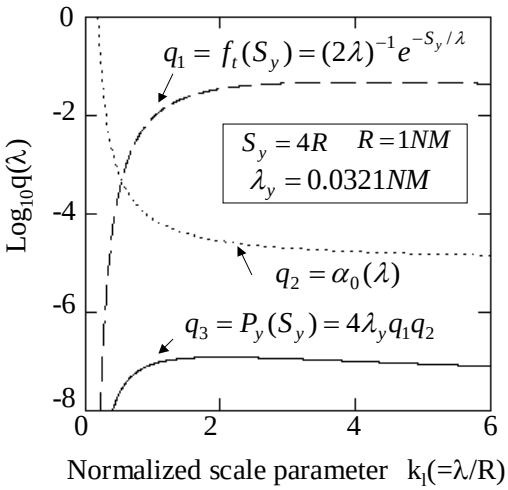

Fig.9 Relation between tail parameter λ and $P_y(S_y)$.

8 Discussion

In the previous chapter we only dealt with the DE tail model. However, we have no information about the true tail distribution at this moment. As a most conservative model for the non-increasing (flattish or decreasing with the magnitude of cross track error) tail distribution, let us consider a uniform distribution for $f_t(x)$.

In the case of a uniform tail distribution, $P_y(S_y)$ depends on the length of the tails. From the consideration in the previous paper [3], we can understand intuitively that the most conservative case is that one tail on one track covers the whole core region of the other track. Then, the pdf model of the uniform tail can be given by

$$f_t(x) = \begin{cases} 1/(2L) & for \quad |x| \le L = S_y + 2R \\ 0 & otherwise \end{cases} \qquad (41)$$

Eq.(20) and Eq.(21) can be satisfied regardless of the distribution types for the core and the tail. Eq.(37) is also not limited to the DE tail model. Accordingly, plugging Eq.(41) into Eq.(37), we obtain α_0 for the above uniform tail. This is given by

$$\alpha_0 = L\gamma_2 / S_y \qquad (42)$$

Then, the value of $P_y(S_y)$ for the uniform tail model is given by

$$P_y(S_y)_{uniform} \approx 4\lambda_y \alpha_0 f_t(S_y) = 2\lambda_y \gamma_2 / S_y \qquad (43)$$

Table 1 compares the simple expressions of the maximum lateral overlap probability for each model. These can be expressed as a function of four essential parameters, i.e., the route spacing S_y , RNP value R, the probability of large cross track errors associated with the containment limit γ_2 and the average wing span of aircraft λ_y .

Accordingly, the ratio of the maximum lateral overlap probabilities for the DE and uniform tail models is given by

$$\frac{P_y(S_y)_{uniform}}{P_y(S_y)_{DE}} = \frac{(S_y - 2R)\cdot e}{S_y} \qquad (44)$$

In case of $S_y = 4R$, the ratio becomes very simple, i.e., $e/2 \approx 1.36$. This means that the maximal overlap probability for t $P_y(S_y)$ the uniform tail model is about 1.4 times greater than for the DE tail model.

Table 1 Comparison of maximum lateral overlap probability for each model.

Tail model	Double Exponential (DE)	Uniform with $L = S_y + 2R$
$f_t(x)$	$\frac{e^{-\lvert x\rvert/\lambda}}{2\lambda}$	$\begin{cases} 1/(2L) & for \quad \lvert x\rvert \le L \\ 0 & otherwise \end{cases}$
α_0	$\gamma_2 e^{2R/\lambda}$	$\frac{\gamma_2 L}{S_y}$
$P_y(S_y)$	$\frac{2\lambda_y \cdot \gamma_2}{(S_y - 2R)e}$	$\frac{2\lambda_y \cdot \gamma_2}{S_y}$

9. Concluding Remarks

This paper proposes a continuous mixture distribution model for cross track errors of the aircraft with RNP alerting capability. Its components are the generalized Laplace (GL) distribution and the double exponential (DE) distribution. For large deviations, a simple expression for the maximum lateral overlap probability was derived. This approximation

was compared with that for a uniform tail model.

The analysis of the lateral overlap probability indicated the following characteristics:
(1) a Gaussian distribution for the overlap probability is not accurate and
(2) for large deviations, the maximum lateral overlap probability for DE tail model is up to 70 % smaller than that for the uniform tail model .

Our results are initial. They involve a large number of parameters. But they motivate the following future work: an analysis of the robustness to other tail distributions than the double exponential distribution. This answers "how conservative" the current models are. And the exact solutions of the maximization problem will be investigated. This requires formal solutions to non-linear constrained optimization problems, but gives the confidence that the results are applicable.

ACKNOWLEDGEMENT

The author is very grateful to Dr. Claus Gwiggner and Dr. Masato Fujita for his discussion and comments on a draft of this paper.

References

[1] Performance Based Navigation Manual [Draft 5.1], Vol.1, ICAO, March 2007

[2] Manual on Required Navigation Performance (RNP), Second Edition, ICAO Doc 9613- AN/937, 1999

[3] Minimum Aviation System Performance Standards: Required Navigation Performance for Area Navigation, RTCA DO-236A, RTCA Inc., Sept. 13, 2000.

[4] Nagaoka S., Estimating the lateral overlap probability for RNP RNAV parallel tracks", *ICAO SASP-WG/WHL/5-WP/29*, Tokyo, May 2004.

[5] Nagaoka S., An alternative double exponential tail model for estimating the lateral overlap probability of aircraft for RNP RNAV parallel tracks, *ICAO SASP-WG/WHL/6-WP/05*, Washington D.C., November, 2004

[6] Air Traffic Services Planning Manual, ICAO Doc 9426-AN/924,Part II,p.II-2-4-19, 1984

Copyright Statement